galaxies

MDPI

Article

Analysis of Multiple Shell Planetary Nebulae Based on HST/WFPC2 Extended 2D Diagnostic Diagrams

Daniela Barría [1,*] and Stefan Kimeswenger [1,2]

[1] Instituto de Astronomía, Universidad Católica del Norte, Av. Angamos 0610, 1240000 Antofagasta, Chile; skimeswenger@ucn.cl
[2] Institut für Astro- und Teilchenphysik, Universität Innsbruck, Technikerstr. 25, 6020 Innsbruck, Austria
* Correspondence: daniela.barria@ucn.cl; Tel.: +54-55-235-5480

Received: 27 June 2018; Accepted: 1 August 2018; Published: 3 August 2018

Abstract: The investigation of gaseous nebulae, emitting in forbidden lines, is often based extensively on diagnostic diagrams. The special physics of these lines often allows for disentangling with a few line ratios normally coupled thermodynamic parameters like electron temperature, density and properties of the photo-ionizing radiation field. Diagnostic diagrams are usually used for the investigation of planetary nebulae as a total. We investigated the extension of such integrated properties towards spatially resolved 2D diagnostics, using Hubble Space Telescope/Wide Field Planetary Camera 2 (HST/WFPC2) narrow band images. For this purpose, we also derived a method to isolate pure Hα emission from the [N II] contamination as normally suffering in the F656N HST/WFPC2 filter.

Keywords: planetary nebulae; stars: AGB and post-AGB; late stage stellar evolution

1. Introduction

According to the standard Interacting Stellar Winds (ISW) model, Planetary Nebula (PN singular, PNe plural) result from the interaction of a fast, hot and, thin wind developed at the post-AGB phase, which compresses and accelerates the dense material ejected during the final AGB phase [1]. While this model can explain the formation of main structures such as the shell and halo in PNe [2–4], it is not able to characterize the observed additional micro structures such as filaments, knots, clumpiness and low ionization outflows (see e.g., [5–7]). Certainly, radiative and dynamical processes taking place in the interaction of the stellar winds [8] might play a significant role in the origin and evolution of such structures, making clear that the mechanism(s) involved in the nebulae formation cannot be as straightforward as the ISW model predicts. In addition, some round/elliptical PNe show extra outer shells and/or halos (see e.g., [9–11]). These so-called Multiple Shell Planetary Nebulae (MSPNe) are then ideal candidates to study both macro and micro structures at PNe.

Mainly thanks to the great detail on HST images, remarkable low ionization structures such as FLIERs (Fast Low Ionization Emission Regions) or LISs (Low Ionization emission line Structures) have been observed in several MSPNe (see e.g., [12–14]). Compared to their neighboring gas, FLIERs and LISs are characterized to show a remarkable enhancement of low ionization species together to different kinematic properties. Some physical parameters such as electron temperature of FLIERs appears slightly but not so different to their surrounding nebular material (see e.g., [12,15–17]). A 3D photoionization modelling of a PN similar in structure to NGC 7009 shows that FLIERs may have chemical abundances similar to the main shell, but different density [18]. LISs, on the other hand, have shown to be less dense than their surroundings [19]. Thus, FLIERs/LISs 'exceptional' ionization properties seem to be associated to either shock regions or ionization fronts [15]. However, 'pure' shock models are not able to explain the entire observed properties of FLIERs [20]. By means of a series of numerical simulations, in [21] the authors predict the emission line spectrum of knots (low-ionization

structures), which agrees approximately with observed spectra when shown in two-line ratio diagnostic diagrams. For different initial conditions, simulations predict for emission spectrum in a range from shock-excited spectra to spectra similar to those of gas in photoionized equilibrium. In [22] the authors studied near-IR H_2 emission from LISs at two PNe (one of them a MSPN). They found that the low ionization structures in these nebulae show similar traits to photodissociation regions.

Under this scenario and looking for a better interpretation of observed properties, we perform a detailed photometric analysis (using narrow band HST images) of three MSPNe. The line ratios log (Hα/[N II]) versus log (Hα/[S II]) has been used in the past to identify photoionized PNe from shocked nebulae, such as those found in supernova remnants or in H II regions. This scheme was first introduced by [23] and refined in [24]. An extension of this diagnostic diagram to two dimensions was first explored by [6]. Moreover, different diagnostic diagrams for spatially resolved PNe have been used in the last years to distinguish shock ionization from photoionization regions (see e.g., [19,21,25–27]). The high spatial resolution of HST images make them a perfect tool to investigate on line emission ratios at the entire surface of nebulae at each region individually. However, the HST/WFPC2 Hα images taken with the F656N filter might be strongly contaminated by [N II] emission. We present here a method to extract the nitrogen line contamination in the HST Hα images, by using the [N II] image taken with the F658N filter (Figure 1). Using these 'pure' Hα images together with [N II] and [S II] in two line ratios, we investigate the general ionization trends of the nebula versus that of the FLIERs and LISs regions in MSPNe.

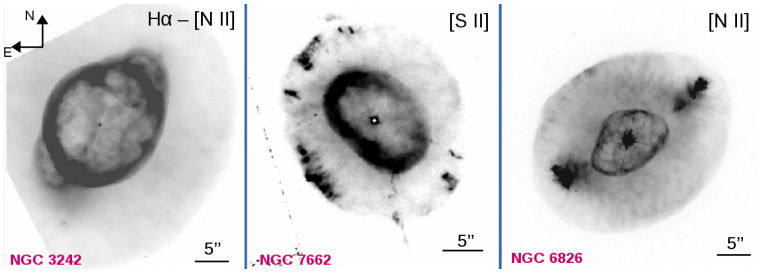

Figure 1. The HST images of some MSPNe. Note that the Hα image of NGC 3242 was already corrected for the contamination of the nitrogen line emission.

2. Methods and Results

The log (Hα/[N II]) versus log (Hα/[S II]) diagnostic diagrams normally were used for spectroscopic results of the nebulae as a total [23,24,28]. As to our knowledge, Reference [6] for the first time used this diagnostics to separate and classify different regions within the PN NGC 2438. There, the data along a long slit spectroscopy was used in detail, to derive a regression line, which then was applied to the entire 2D image from HST. We call these investigations thus thereafter Extended 2D Diagnostic Diagrams (E2DDs).

At this work and by means of HST/WFPC2 images (F656N, F658N, F673N and F502N band filters), we present our outcomes in the analysis of the nebular ionization trend using the E2DD at three MSPNe. We used pre-processed HST/WFPC2 level 2 images, which were flux-calibrated using the IRAF/STSDAS task *imcalc* and sky-subtracted by means of the *sky* task from XVISTA image processing software [29]. As we mentioned, however, the bandwidth of HST/WFPC2 Hα F656N filter include contamination from the [N II] 6583 Å and [N II] 6548 Å lines. Making use of the transmission curves for the F656N filter, we estimated a contamination in the F656N band of 39% for [N II] 6548 Å and 2% for [N II] 6583 Å. In a way to isolate for the Hα emission, we used the F658N filter image, which contains only [N II] 6583 Å, and thus considering for the known line ratio intensity R = ([N II] 6583 Å/[N II] 6548 Å) = 3, we were able to estimate for a total [N II] contribution in the F656N bandpass of 15%. Thus, cleaning the F656N images was possible using this fraction of the flux taken from the F658N image. Hereafter, line ratios for the E2DD were calculated using these 'pure' Hα data. Each image

was then divided in 36 rectangular boxes covering the whole nebula. Each one of these was then sub-divided according to the main fragmentation structures observed in the nebula (see inserts in Figures 2 and 3). In this way, we were able to estimate for line ratios at different sectors and then following on the ionization tendency within each nebulae. Main results (E2DDs) are displayed in Figures 2 and 3. Different colors represent for different main sectors in the nebula. A linear fit to the data is displayed as a black line. Deviating points over a 2σ level were not considered at the fitting.

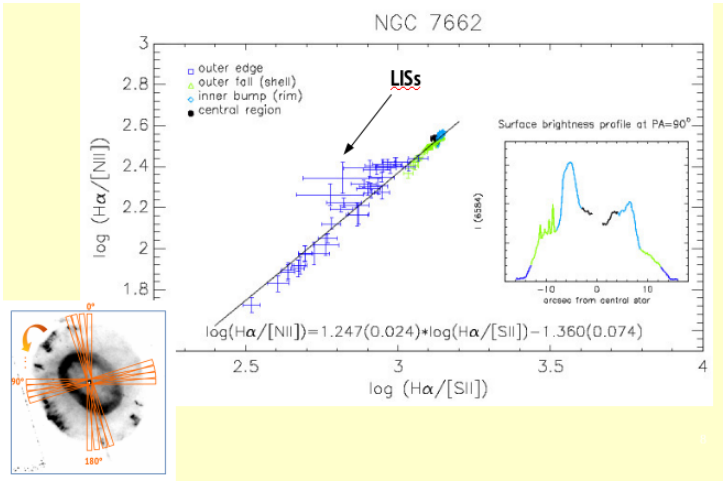

Figure 2. The E2DD derived from sectors of NGC 7662. The bottom-left insert illustrates the method how sectors are arranged in investigating the nebula. Different colors are related to different sectors within the nebula. The right inner plot shows (as an example) the extracted [N II] brightness profile at PA = 90° showing the main fragmentation structures.

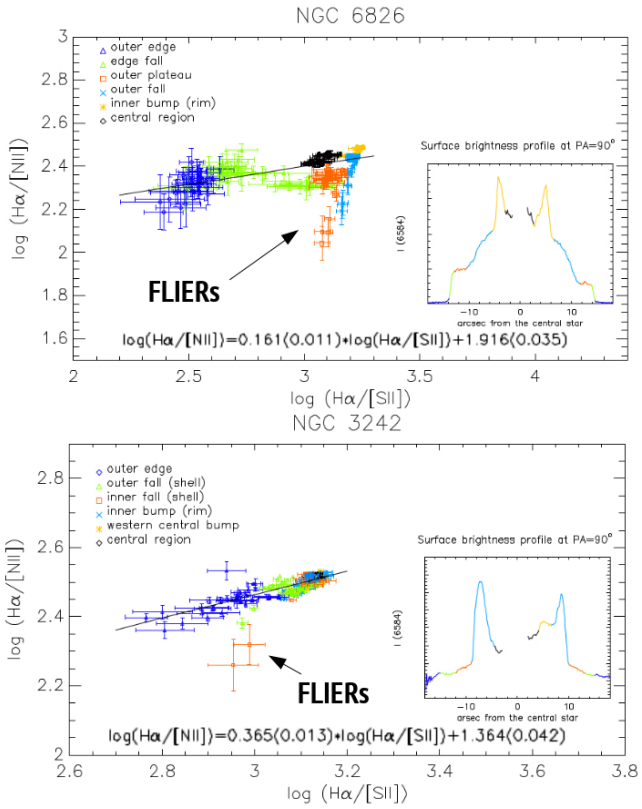

Figure 3. The E2DDs for of a nebula with very pronounced FLIERS and one with very weak ones.

3. Discussion and Conclusions

After careful inspection on the E2DD displayed in Figures 2 and 3, we observe that major deviations from the inside to outside excitation tendency seem to arrive only from regions where FLIERs or LISs are placed. From the outer edge (shell) at NGC 7662, the lower ionization contribution from LISs (compared to the surrounding nebular gas) slightly deviates from the main ionization tendency of the gas. In particular, this nebula exhibits the steepest ionization trend in our sample. On the other hand, showing the lowest inclination trend, NGC 6826 presents significant deviations from the general tendency emerging from the outer regions of the shell (so-called the outer plateau and outer fall at Figure 2). We notice at these regions of the nebula the presence of pronounced FLIERs (see the right-panel at Figure 1). Finally, the low ionization contribution from FLIERs at NGC 3242 becomes clear in its E2DD (Figure 3). Here, moderate deviating points emerge from the external regions of the shell where weak FLIERs are located.

Considering these outcomes, we conclude that no additional deviating data points beyond the ones related to FLIERs or LISs presence has been detected in the E2DD at this small MSPNe sample. If we assume that regions without the influence of FLIERs or LISs are dominated by photoionization as the main excitation mechanism, the influence of further processes could be affecting regions were these low ionization emission structures are present.

On the other hand, the three MSPNe investigated here exhibit similar properties like slight sub-solar abundances, high range of excitation, small expansion velocities and similar kinetic ages. Thus, we wonder about the strong differences observed at the inclination of the main ionization trend. Some open questions thus arise: do and, if so, how do the CSPNe parameters affect the inclination of the ionization trends? Moreover, is there any correlation between the properties of FLIERs (or LISs) and the ionization tendency of the surrounding gas? Why FLIERs/LISs can show different locations in the E2DD (below or above the main ionization trend)?

On the other hand, the presence of low ionization structures has been advertised as an indicator for central star binarity (see e.g., [30] and references therein). The fast rotating central star of NGC 6826 has been shown to be product of a binary evolution [31]. At this point, we wonder if this fact is somehow correlated to the lowest ionization tendency we observe in this nebula. As a future work, it becomes necessary to explore, using a bigger and more diversified sample of MSPNe, to study their E2DD ionization trends and its possible correlation to the stellar and/or nebular parameters.

Author Contributions: Conceptualization, D.B. and S.K.; Investigation, D.B.; Writing—Original Draft Preparation, D.B.; Writing—Review & Editing, D.B. and S.K.; Project Administration, D.B.; Funding Acquisition, S.K.

Funding: This research was funded by FONDO ALMA-Conicyt Programa de Astronomía/PCI 31150001.

Acknowledgments: Data used in this paper were based on observations made with the NASA/ESA Hubble Space Telescope, and obtained from the Hubble Legacy Archive, which is a collaboration between the Space Telescope Science Institute (STScI/NASA), the Space Telescope European Coordinating Facility (ST-ECF/ESA) and the Canadian Astronomy Data Centre (CADC/NRC/CSA). HST archival images were taken under proposal program ID 6117 (P.I. Bruce Balick). This research has made use of the SIMBAD database, operated at CDS, Strasbourg, France. We kindly thank the conference organizers for their help and Martin Guerrero and Quentin Parker for helpful discussion.

Conflicts of Interest: The authors declare no conflict of interest.

References

1. Kwok, S.; Purton, C.R.; Fitzgerald, P.M. On the origin of planetary nebulae. *Astrophys. J.* **1978**, *219*, L125–L127. [CrossRef]
2. Schönberner, D.; Steffen, M. Planetary Nebulae with Double Shells and Haloes: Insights from Hydrodynamical Simulations. *Rev. Mex. Astron. Astrofis.* **2002**, *12*, 144–145.
3. Perinotto, M.; Schönberner, D.; Steffen, M.; Calonaci, C. The evolution of planetary nebulae. I. A radiation-hydrodynamics parameter study. *Astron. Astrophys.* **2004**, *414*, 993–1015. [CrossRef]
4. Schönberner, D. The dynamical evolution of planetary nebulae. *J. Phys. Conf.* **2016**, *728*, 032001. [CrossRef]

5. Matsuura, M.; Speck, A.K.; McHunu, B.M.; Tanaka, I.; Wright, N.J.; Smith, M.D.; Zijlstra, A.A.; Viti, S.; Wesson, R. A "Firework" of H_2 Knots in the Planetary Nebula NGC 7293 (The Helix Nebula). *Astrophys. J.* **2009**, *700*, 1067–1077. [CrossRef]
6. Öttl, S.; Kimeswenger, S.; Zijlstra, A.A. Ionization structure of multiple-shell planetary nebulae. I. NGC 2438. *Astron. Astrophys.* **2014**, *565*, A87. [CrossRef]
7. Fang, X.; Guerrero, M.A.; Miranda, L.F.; Riera, A.; Velázquez, P.F.; Raga, A.C. Hu 1-2: A metal-poor bipolar planetary nebula with fast collimated outflows. *Mon. Not. R. Astron. Soc.* **2015**, *452*, 2445–2462. [CrossRef]
8. García-Segura, G.; López, J.A.; Steffen, W.; Meaburn, J.; Manchado, A. The Dynamical Evolution of Planetary Nebulae after the Fast Wind. *Astrophys. J. Lett.* **2006**, *646*, L61–L64. [CrossRef]
9. Gómez-Muñoz, M.A.; Blanco Cárdenas, M.W.; Vázquez, R.; Zavala, S.; Guillén, P.F.; Ayala, S. Morpho-kinematics of the planetary nebula NGC 3242: An analysis beyond its multiple-shell structure. *Mon. Not. R. Astron. Soc.* **2015**, *453*, 4175–4184. [CrossRef]
10. Guerrero, M.A.; Manchado, A. On the Chemical Abundances of Multiple-Shell Planetary Nebulae with Halos. *Astrophys. J.* **1999**, *522*, 378–386. [CrossRef]
11. Corradi, R.L.M.; Steffen, M.; Schönberner, D.; Jacob, R. A hydrodynamical study of multiple-shell planetary nebulae. II. Measuring the post-shock velocities in the shells. *Astron. Astrophys.* **2007**, *474*, 529–539. [CrossRef]
12. Balick, B.; Alexander, J.; Hajian, A.R.; Terzian, Y.; Perinotto, M.; Patriarchi, P. FLIERs and Other Microstructures in Planetary Nebulae. IV. Images of Elliptical PNs from the Hubble Space Telescope. *Astron. J.* **1998**, *116*, 360–371. [CrossRef]
13. García-Díaz, M.T.; López, J.A.; Steffen, W.; Richer, M.G. A Detailed Morpho-kinematic Model of the Eskimo, NGC 2392: A Unifying View with the Cat's Eye and Saturn Planetary Nebulae. *Astrophys. J.* **2012**, *761*, 172. [CrossRef]
14. Gonçalves, D.R.; Corradi, R.L.M.; Mampaso, A.; Quireza, C. Do the Various Types of PNe Knots Differ in Terms of their Physical Properties? The case of NGC 7662. *Rev. Mex. Astron. Astrofis.* **2009**, *35*, 64–65.
15. Balick, B.; Rugers, M.; Terzian, Y.; Chengalur, J.N. Fast, low-ionization emission regions and other microstructures in planetary nebulae. *Astrophys. J.* **1993**, *411*, 778–793. [CrossRef]
16. Balick, B.; Perinotto, M.; Maccioni, A.; Terzian, Y.; Hajian, A. FLIERs and other microstructures in planetary nebulae, 2. *Astrophys. J.* **1994**, *424*, 800–816. [CrossRef]
17. Danehkar, A.; Parker, Q.A.; Steffen, W. Fast, Low-ionization Emission Regions of the Planetary Nebula M2-42. *Astron. J.* **2016**, *151*, 38. [CrossRef]
18. Gonçalves, D.R.; Ercolano, B.; Carnero, A.; Mampaso, A.; Corradi, R.L.M. On the nitrogen abundance of fast, low-ionization emission regions: the outer knots of the planetary nebula NGC 7009. *Mon. Not. R. Astron. Soc.* **2006**, *365*, 1039–1049. [CrossRef]
19. Akras, S.; Gonçalves, D.R. Low-ionization structures in planetary nebulae-I. Physical, kinematic and excitation properties. *Mon. Not. R. Astron. Soc.* **2016**, *455*, 930–961. [CrossRef]
20. Riera, A.; Raga, A.C. Physical conditions of the shocked regions in collimated outflows of planetary nebulae. In Proceedings of the Asymmetrical Planetary Nebulae IV, La Palma, Spain, 18–22 June 2007.
21. Raga, A.C.; Riera, A.; Mellema, G.; Esquivel, A.; Velázquez, P.F. Line ratios from shocked cloudlets in planetary nebulae. *Astron. Astrophys.* **2008**, *489*, 1141–1150. [CrossRef]
22. Akras, S.; Gonçalves, D.R.; Ramos-Larios, G. H_2 in low-ionization structures of planetary nebulae. *Mon. Not. R. Astron. Soc.* **2017**, *465*, 1289–1296. [CrossRef]
23. Garcia Lario, P.; Manchado, A.; Riera, A.; Mampaso, A.; Pottasch, S.R. IRAS 22568 + 6141—A new bipolar planetary nebula. *Astron. Astrophys.* **1991**, *249*, 223–232.
24. Magrini, L.; Perinotto, M.; Corradi, R.L.M.; Mampaso, A. Spectroscopy of planetary nebulae in M 33. *Astron. Astrophys.* **2003**, *400*, 511–520. [CrossRef]
25. Gonçalves, D.R.; Mampaso, A.; Corradi, R.L.M.; Quireza, C. Low-ionization pairs of knots in planetary nebulae: Physical properties and excitation. *Mon. Not. R. Astron. Soc.* **2009**, *398*, 2166–2176. [CrossRef]
26. Ali, A.; Dopita, M.A. IFU Spectroscopy of Southern Planetary Nebulae V: Low-Ionisation Structures. *Publ. Astron. Soc. Aust.* **2017**, *34*, e036. [CrossRef]
27. Danehkar, A.; Karovska, M.; Maksym, W.P.; Montez, R., Jr. Mapping Excitation in the Inner Regions of the Planetary Nebula NGC 5189 Using HST WFC3 Imaging. *Astrophys. J.* **2018**, *852*, 87. [CrossRef]

28. Frew, D.J.; Parker, Q.A. Planetary Nebulae: Observational Properties, Mimics and Diagnostics. *Publ. Astron. Soc. Aust.* **2010**, *27*, 129–148. [CrossRef]
29. Barría, D.; Kimeswenger, S. HST/WFPC2 imaging analysis and Cloudy modelling of the multiple shell planetary nebulae NGC 3242, NGC 6826 and NGC 7662. *Mon. Not. R. Astron. Soc.* **2018**. [CrossRef]
30. Jones, D.; Boffin, H.M.J. Binary stars as the key to understanding planetary nebulae. *Nat. Astron.* **2017**, *1*, 0117. [CrossRef]
31. De Marco, O.; Long, J.; Jacoby, G.H.; Hillwig, T.; Kronberger, M.; Howell, S.B.; Reindl, N.; Margheim, S. Identifying close binary central stars of PN with Kepler. *Mon. Not. R. Astron. Soc.* **2015**, *448*, 3587–3602. [CrossRef]